Carbohydrate Polymers 80 (2010) 186–196

Contents lists available at ScienceDirect

Carbohydrate Polymers

journal homepage: www.elsevier.com/locate/carbpol

Estimation of the surface accessible inclusion sites of β-cyclodextrin based copolymer materials

Mohamed H. Mohamed [a], Lee D. Wilson [a,*], John V. Headley [b]

[a] Department of Chemistry, 110 Science Place (Rm. 156), University of Saskatchewan, Saskatoon, SK, Canada S7N 5C9
[b] Aquatic Ecosystems Protection Research Division, Water Science and Technology Directorate, 11 Innovation Boulevard, Saskatoon, SK, Canada S7N 3H5

ARTICLE INFO

Article history:
Received 25 September 2009
Received in revised form 4 November 2009
Accepted 9 November 2009
Available online 13 November 2009

Keywords:
Copolymers
Cyclodextrin
Inclusion complexes
Phenolphthalein
Polyurethanes

ABSTRACT

Aqueous solutions containing insoluble β-cyclodextrin (β-CD) based urethane copolymers were studied in aqueous solutions by measuring the absorbance changes (decolourization) of phenolphthalein (phth) at pH 10.5. The various copolymers were comprised of β-CD and five diisocyanate linkers (1,6-hexamethylene diisocyanate (HDI), 4,4′-dicyclohexyl diisocyanate (CDI), 4,4′-diphenylmethane diisocyanate (MDI), 1,4-phenylene diisocyanate (PDI), and 1,5-naphthalene diisocyanate (NDI)). The copolymers studied were prepared at the β-CD: linker reactant ratios 1:1, 1:2, and 1:3, respectively. The decolourization studies provided estimates of the 1:1 binding constants (K_1) for the monomer β-CD/phth inclusion complex. It was concluded that the values of K_1 for copolymer/phth systems for highly accessible β-CD inclusion sites in copolymer materials closely resembles the K_1 value for the 1:1 β-CD/phth complex. The surface accessibility of the β-CD inclusion binding sites for the copolymers ranged from 1-100%. The observed variability was attributed to steric effects in the annular hydroxyl region of β-CD and the relative accessibility of the micropore sites within the polymer framework as a consequence of the variable cross linking. The Gibbs free energy of complex formation (ΔG°) and site occupancy (θ) of phth adsorbed to the copolymer materials was estimated independently using the Sips isotherm model. The ΔG° values ranged between -27 and -30 kJ mol^{-1} and are in agreement with the Gibbs free energy for the 1:1 β-CD/phth complexes (~ -27 kJ mol^{-1}). The phth decolourization technique provides a simple, low cost and versatile method for the estimation of the surface accessible inclusion sites of β-CD in CD based urethane copolymer materials. This method is anticipated to have extensive analytical applications in materials research and for the design of functional β-CD based sorbent materials.

1. Introduction

Cyclodextrins (CDs) are cyclic compounds consisting of six, seven, or eight α-D-glucopyranose units connected by α-(1→4) linkages commonly referred to as α-, β-, and γ-CDs, respectively (Bender & Komiyama, 1978). CDs possess a characteristic toroidal shape with a well-defined lipophilic cavity and a hydrophilic exterior that is suitable for the inclusion binding of appropriate sized guest compounds (cf. Scheme 1). CDs are of interest, in part, because of their ability to form stable inclusion complexes in aqueous solution (Buvari, Szejtli, & Barcza, 1983; Eftink, Andy, Bystrom, Perlmutter, & Kristol, 1989; Georgiou, Georgiou, & Koupparis, 1995; Mohamed, Wilson, Headley, & Peru, 2009; Taguchi, 1986; Wilson, Siddall, & Verrall, 1997).

Recently, β-CD has been incorporated into cross linked polymeric forms using a variety of linker molecules (e.g., epichlorohydrin, glutaraldehye, succinyl chloride, diisocyanates, diacid chlorides, dicarboxylic acids, cyanuric chloride) (Wenz, 1994; Crini et al., 1998; Harada, Hashidzume, & Takashima, 2006; Mohamed, Wilson, Headley, & Peru, 2008; Mohamed et al., 2009). These types of copolymer materials have been utilized for the sequestration of organic compounds from the gas and condensed phases. The determination of the number and availability of inclusion sites is an important parameter for the characterization of the sorption properties β-CD based copolymer materials. The surface area and pore structure characteristics are important physiochemical properties known to affect the sorption properties of porous polymeric materials; particularly for amorphous and non-templated materials (Crini, 2005). Estimation of the available inclusion sites is anticipated to provide an understanding of the relative role of β-CD inclusion sites and the linker domains in the sorption mechanism, particularly for heterogeneous polymer sorption in aqueous solution. Porosimetry provides estimates of all the surface accessible regions (micropores to macropores), however; backfill gases (e.g., nitrogen or argon) are not selectively bound to different adsorption sites. In contrast, techniques such as XRD are less discriminatory and provide estimates of the total surface accessible and inaccessi-

* Corresponding author. Tel.: +1 306 966 2961; fax: +1 306 966 4730.
E-mail address: lee.wilson@usask.ca (L.D. Wilson).

0144-8617/$ - see front matter © 2009 Elsevier Ltd. All rights reserved.
doi:10.1016/j.carbpol.2009.11.014

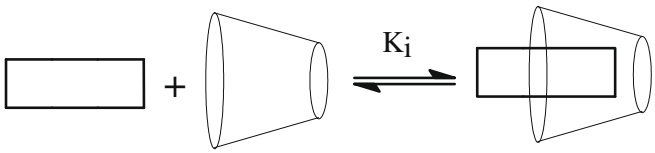

Scheme 1. The formation of an host-guest complex is shown for a β-CD (toroid) and a guest molecule (rectangle) according to an equilibrium process where K_i is the 1:1 equilibrium binding constant and the solvent has been omitted for clarity.

ble pores. Solution based dye sorption methods provide complementary information about the surface accessible regions (e.g., inclusion and linker domains) of β-CD based copolymer materials.

Binding constants of β-CD inclusion complexes have been previously estimated using direct and indirect methods. Direct methods typically involve the measurement of the concentration of bound or unbound guest molecules and include methods such as ^{1}H NMR (Wood, Hruska, & Saenger, 1977), sound velocity (Junquera, Tardajos, & Aicart, 1993), conductivity (Saint Aman & Serve, 1990), surface tension (Dharmawardana, Christian, Tucker, Taylor, & Scamehorn, 1993), electrochemical measurements (Wan Yunus, Taylor, Bloor, Hall, & Wyn-Jones, 1992), UV–vis (Gelb, Schwartz, Cardelino, & Laufer, 1980), and fluorescence spectrophotometry (Fourmentin et al., 2006). Spectrophotometric methods (Buvári & Barcza, 1979; Harrison & Eftink, 1982; Selvidge & Eftink, 1986; Buvári, Barcza, & Kajtár, 1988; Sasaki, Christian, & Tucker, 1989; Gray, MacLean, & Reinsborough, 1995; Meier, Luiz, Farmer, & Szpoganicz, 2001; Tutaj, Kasprzyk, & Czapkiewicz, 2003; Fourmentin et al., 2006), employ the measurement of absorbance changes of suitable organic dyes such as phenolphthalein (phth), methyl orange (MO) and *p*-nitrophenol (PNP) in the presence of a host molecule (Buvári & Barcza, 1979; Harrison & Eftink, 1982; Selvidge & Eftink, 1986; Buvári et al., 1988; Sasaki et al., 1989; Gray et al., 1995; Landy, Fourmentin, & Surpateanu, 2000; Meier et al., 2001; Tutaj et al., 2003; Suzuki & Yamauchi, 2006). Phenolphthalein is a preferred chromophoric dye in UV–vis spectrophotometry because it exhibits molecular recognition with β-CD as evidenced by its specific inclusion geometry (Buvari et al., 1983; Georgiou et al., 1995; Taguchi, 1986), and a relatively large 1:1 binding constant ($K_1 \sim 10^4\,M^{-1}$) (Buvári & Barcza, 1979; Selvidge & Eftink, 1986; Buvári et al., 1988; Sasaki et al., 1989; Gray et al., 1995; Tutaj et al., 2003).

Characterization of the sorption properties of microporous copolymer materials containing β-CD involves an estimation of the surface accessible binding sites (Janus et al., 1999; Topchieva et al., 2003; Wintgens & Amiel, 2005; Velaz, Isasi, Sanchez, Uzquenda, & Ponchel, 2007; Burckbuchler et al., 2008; Rossi, Silva, Vico, & Gonzalez, 2009;). The ability to measure the accessible β-CD inclusion sites is necessary when designing suitable sorbent materials that require inclusion binding for specialized applications. Recent studies have examined the interaction between phenolphthalein (phth) and β-CD copolymer materials; however, no detailed quantitative studies were reported at the time of this publication (Topchieva et al., 2003; Velaz et al., 2007; Bergamasco, Zanin, & Moraes, 2007; Fontananova, Di Profio, Curcio, Giorno, & Drioli, 2007; Uyar et al., 2009). Studies that utilize phth as a probe for the analysis of polymeric materials containing β-CD groups have been reported (Topchieva et al., 2003; Velaz et al., 2007; Bergamasco et al., 2007; Fontananova et al., 2007; Uyar et al., 2009). Topchieva et al. estimated the number of binding sites for β-CD based nanotubes; however, the use of a non-zero molar absorptivity (ε) for the bound form of phth (*i.e.* β-CD/phth) in the equilibrium binding model is inconsistent with the parameter estimates ($\varepsilon \approx 0$) reported by other researchers, *vide infra*. Velaz et al. concluded that the changes in the absorbance of phth provided evidence of the limited accessibility of the β-CD inclusion sites in their polymer materials. Fontanova et al. indicated that the accessibility and binding sites of the β-CD polymers may be estimated using the decolourization of phth (Fontananova et al., 2007) while Uyar et al. recently reported the degree of decolourization of β-CD based composite polystryrene fibers.

In this paper, we report a detailed quantitative study of the estimation of the surface accessible β-CD inclusion sites for a systematic series of urethane based copolymer materials. As well, we conclude that the 1:1 binding constants for the β-CD inclusion sites in copolymer/phth systems with relatively high accessibility are similar to those of native β-CD. The 1:1 binding constants decrease as the relative accessibility of β-CD decreases. The copolymers investigated are urethanes comprised of β-CD and five types of diisocyanate cross linker molecules at 1:1, 1:2, and 1:3 reactant (β-CD:linker) mole ratios, respectively. The diisocyanates are as follows: 1,6-hexamethylene diisocyanate (HDI), 4,4′-dicyclohexyl diiscoyanate (CDI), 4,4′-diphenylmethane diisocyanate (MDI), 1,4-phenylene diisocyanate (PDI), and 1,5-naphthalene diisocyanate (NDI). Finally, the importance and application of this dye based method will be discussed.

2. Experimental

2.1. Materials

Dimethylacetamide (DMA) DriSolv 99.8%min (EMD), methanol, chromasolv for HPLC, ⩾99.9% (Sigma–Aldrich) and ethyl ether anhydrous (EMD) were used at different stages of polymer preparation. Phosphorous pentoxide, P_2O_5 (BDH Chemicals Ltd.) was used for drying β-CD. Phenolphthalein, phth (BDH Chemicals Ltd.), sodium hydrogen carbonate (BDH Chemicals Ltd.) and sodium hydroxide (Alfa Aesar) was used to prepare aqueous phth dye solutions.

2.2. Polymer preparation

A procedure for the synthesis of urethane based β-CD materials was adopted from our previous work with an additional Soxhlet extraction step after methanol with ethyl ether (Mohamed et al., 2008). Polymers of β-cyclodextrin, β-CD (VWR) and D(+)-glucose monohydrate (EMD) were synthesized via cross linking reactions with diisocyanate cross linker molecules. These linkers include the following; HDI (Fluka), CDI (Aldrich), MDI (Aldrich), PDI (Aldrich) and NDI (TCI).

2.3. Polymer characterization

Solid-state ^{13}C NMR spectroscopy was performed using cross polarization (CP; ^{13}C {^{1}H}) with magic angle spinning (MAS). ^{13}C NMR spectra were run at 150.8 MHz on a Varian Inova-600 NMR spectrometer with a 3.2 mm rotor, spinning rate 16 kHz with a cp (^{13}C {^{1}H}) ramp pulse program. The chemical shifts were externally referenced to hexamethyl benzene at 16.9 ppm at ambient temperature. Data were processed with a 100 Hz line broadening with left shifting of the FID (1–2 data points) to correct the spectral baseline. IR reflection spectra were obtained with a BIO-RAD FTS-40 spectrophotometer. Spectroscopic grade KBr was used as both the background and matrix over the range of 400–4000 cm^{-1}. Samples were prepared by mixing with pure spectroscopic grade KBr in appropriate amounts and ground in a small mortar and the powders were subsequently analyzed. The spectra were recorded in a diffuse reflectance mode (with Fourier Transform processing) at room temperature with a 4 cm^{-1} resolution and multiple scans. The content (w/w, %) of carbon (C), hydrogen (H), and nitrogen (N) was measured by Perkin-Elmer 2400 CHN Elemental Analyzer

with a detection limit ±0.3%. The results were uncorrected according to the estimated water/solvent content. The presence of water/solvent mixtures in the polymers was confirmed by ^{1}H NMR (500 MHz Bruker), and ^{13}C NMR for water soluble and insoluble materials, respectively. The residual solvent content (e.g., water and DMA) was estimated using a thermogravimetric analyzer, TGA (Q50 TA Instruments).

2.4. Solution preparation

All solutions were prepared by volume in a 0.1 M sodium hydrogen carbonate buffer adjusted to pH 10.5 with 6 M sodium hydroxide. The concentration of phth (C_{phth}) was maintained at $\sim 3.6 \times 10^{-5}$ M in all experiments. A stock solution of phth in ethanol was made and aliquots were utilized to prepare aqueous solutions of phth in buffer. The ethanol/water (0.04%; v/v) (Wilson et al., 1997), solution was used to increase the solubility of phth. All aqueous solutions were freshly prepared and run within 24 h to ensure that absorbance changes due to any instability of phth did not contribute to experimental artefacts. All absorption measurements were carried out at $\lambda = 552$ nm and no change in the shape of the visible absorption band with increasing concentration of β-CD ($C_{\beta\text{-CD}}$) was observed at this wavelength.

2.5. Polymer sorption

Seven milliliters of aqueous solution containing phth ($\sim 3.6 \times 10^{-5}$ M) were added to vials containing variable mass amounts of sorbent (e.g., β-CD, glucose, glucose copolymer and CD copolymers). The mixtures were shaken for 24 h, centrifuged (Precision Micro-Semi Micro Centricone, Precision Scientific Co.) at 1550 rpm, and the absorbance of the supernatant was measured using a double beam spectrophotometer (Varian CARY 100) at room temperature (295 ± 0.5 K) to monitor the absorbance changes at λ_{max} of 552 nm.

2.6. Data analysis

A previously described (Wilson et al., 1997) non-linear least squares (NLLS) fitting procedure was used to determine the 1:1 equilibrium binding constants (K_1) between β-CD and phth. The method utilizes the Beer-Lambert law and the assumption that the molar absorptivity of the β-CD/phth complex is zero (Buvari et al., 1983; Taguchi, 1986; Eftink et al., 1989). The formation of the 1:1 complex for β-CD and phth t equilibrium, and the mass-balance relations are given below

$$\beta\text{-CD} + \text{phth} \overset{K_1}{\rightleftarrows} \beta\text{CD/phth} \tag{1}$$

$$[\text{phth}]_0 = [\text{phth}] + [\text{CD-phth}] = [\text{phth}](1 + K_1[\text{CD}]) \tag{2}$$

$$[\text{CD}]_0 = [\text{CD}] + [\text{CD-phth}] \tag{3}$$

The terms $[CD]_0$, [CD], and [CD-phth] refer to the total, unbound, and 1:1 complexed forms of β-CD, respectively. The 1:1 equilibrium binding constant (K_1) for β-CD and phth is expressed as follows

$$[\text{CD-phth}] = [\text{phth}]_0 \left(1 + \frac{1}{K_1[\text{CD}]}\right)^{-1} \tag{4}$$

The values for [CD-phth] and [phth] were obtained using the Beer-Lambert law for phth and Eqs. (2) and (3). The estimates of K_1 using Eq. (4) employ the Beer-Lambert law for the unbound fraction of phth and the assumption that the molar absorptivity of the β-CD/phth complex is zero (Buvari et al., 1983; Taguchi, 1986; Eftink et al., 1989). The criterion utilized for the best fit in the NLLS procedure involved the minimisation of the sums of the squares of the residuals (SSR) according to the relation, $SSR = \sum_i [(A_{calc})_i - (A_{expt})_i]^2$ where A_{calc} and A_{expt} are the calculated and experimental absorbance values, respectively.

The site occupancy (θ) for phth onto the polymer framework and ΔG° values for sorption (complex formation) were determined independently as fitting parameters, Q_m and K_{eq}, from the Sips equilibrium isotherm (Sips, 1948; Liu & Liu, 2008), according to Eq. (5). The Sips model accounts for the heterogeneity of the adsorbents and the interactions with the adsorbed layer. This model provides a better fit over the Langmuir model and reaffirms that other sorption sites and modes of interaction for phth may contribute apart from the β-CD inclusion sites. The contribution of non-inclusion polymer/phth interactions is not anticipated to be significant; however, they are taken into account with the Sips isotherm model.

$$Q_e = Q_m \frac{K_{eq} C_e^{n_s}}{1 + K_{eq} C_e^{n_s}} \tag{5}$$

Q_e is the amount of phth adsorbed by the polymer (mol phth/g copolymer), Q_e is the maximum amount of phth adsorbed by the polymer, C_e is the equilibrium amount of phth in aqueous solution (M), K_{eq} is the 1:1 equilibrium binding constant (M^{-1}), and n_s is the Sips constant (where $n_s > 1$). It is worth to note that the Sips model converges with the Langmuir model when n_s is equal to unity for homogenous sorption processes. The fractional site occupancy of the adsorbate and the corresponding ΔG° of complex formation are defined as follows

$$\theta = \frac{Q_e}{Q_m} \tag{6}$$

$$\Delta G^\circ = -RT \ln K_{eq} \tag{7}$$

R is the gas constant ($Jmol^{-1}\ K^{-1}$), T is temperature in K, and K_{eq} is defined as in Eq. (5). The Sips parameters are forthwith interpreted in terms of the formation of 1:1 β-CD/phth inclusion complexes (cf. Eq. (1)); where $K_{eq} \approx K_1$.

3. Results and discussion

3.1. Characterization of the CD polymers

^{13}C solid state NMR and IR have been reported previously where the copolymer materials (e.g., CD-PDI copolymer) were fully characterized (Mohamed et al., 2008). In this work, additional urethane copolymer materials were investigated and the corresponding ^{13}C CP-MAS spectra are included in Fig. 1. Fig. 1a-f illustrate typical ^{13}C solids NMR spectra observed for the CD-based polymers with variable diisocyanate linker units at a fixed mole ratio (*i.e.*, NDI, PDI, MDI, CDI and HDI) along with the native β-CD precursor. Although each glucose unit of β-CD contains six unique C atoms, the spectrum for β-CD in Fig. 1a reveals four ^{13}C NMR lines between 60 and 110 ppm due to overlap of some of the carbon signatures. The assignment and spectrum reported here agrees with previous reports. As observed in Fig. 1b–f, ^{13}C signatures are observed for β-CD and the various types of aliphatic (cf. 20-70 ppm) and aromatic (cf. 110-170 ppm) linker molecules, respectively. In comparison to the ^{13}C NMR signals of native β-CD and the diisocyanates (results not shown), the urethane copolymers exhibit broader line widths, as is often observed in such amorphous CD based copolymer materials. The decreased crystallinity observed in the ^{13}C NMR spectra is related to the random attachment of the diisocyanate linker molecules to the various hydroxyl group positions (C_2, C_3, and C_6) of β-CD (*vide infra*) and the differences in cross polarization dynamics of the copolymer urethane materials as compared with native β-CD hydrate.

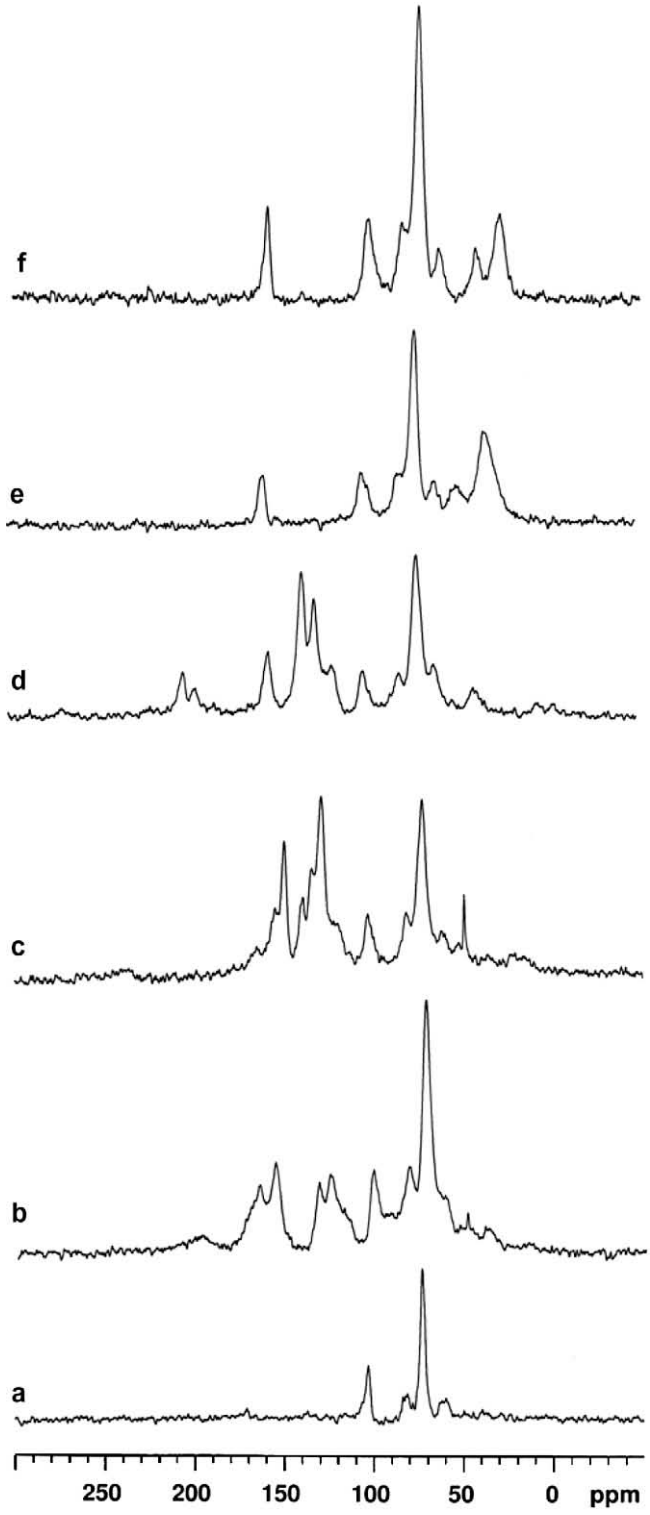

Fig. 1. ^{13}C CP-MAS NMR spectra of CD copolymer materials recorded at ambient temperature, 16 kHz spinning speed, and 150.8 MHz: The spectra are listed as follows: (a) β-CD, (b) NDI-3, (c) PDI-3, (d) MDI-3, (e) CDI-3, and (f) HDI-3.

Elemental analyses provided estimates of the linker composition since the N content increased as the linker ratio increased, as shown in Table 1. Corrections due to water and/or solvent mixtures within the copolymers after extensive drying under vacuum were not applied due to a lack of quantitative estimates of the relative amounts of residual solvent in the products. However, the total contribution of solvent varied from ~0.3–2% as indicated by TGA. The presence of water/solvent contributions was confirmed with ^{1}H NMR spectra where DMA and water signatures were observed (results not shown). The occurrence of trace solvent residues was attributed to the occlusion of solvent within the polymer framework during copolymer formation. The elemental analyses in Table 1 for the theoretical composition of β-CD and glucose were corrected by varying the hydrate water content. Whilst the percentages of C and N increase as expected, H does not decrease as predicted and corrections due to presence of hydrate water result in better agreement between experimental and the calculated values.

3.2. Sorption of phenolphthalein

A low ethanol composition (0.04% (v/v)) was chosen to eliminate possible interferences due to competitive binding by ethanol and to limit undue solvent effects (Donze, Chatjigakis, & Coleman, 1992; Warner & Schuette, 1993; Schuette & Warner, 1994; Wilson et al., 1997). The solution pH at 10.5 was chosen in order to optimize ε_{phth}, to provide greater sensitivity for absorption measurements, and to minimize the potential for deprotonation of the hydroxyl groups of β-CD (p*K*a ≅ 12). The equilibrium structures of the phth dianions in aqueous solution are shown in Scheme 2.

Bertau and Jorg previously studied the interaction of low molecular weight saccharides with phth and it was concluded that decolourization of phth was induced. Decolourization was attributed to non-specific enclathration and H-bonding interactions between the saccharides and phth suggests that the potential of phth as an inclusion specific probe may be limited. To evaluate any potential interferences, a glucose based urethane copolymer was synthesized (*i.e.* glucose:CDI (1:3)) and the nature of the polymer interactions with phth were studied. Fig. 2 illustrates the change in absorbance (Abs) of phth against the mole concentration of glucose for a glucose:CDI (1:3) copolymer. There is a minor but gradual decolourization of phth (~0.1 absorbance units) over a 10 mM concentration range. The weak interaction of phth with glucose:CDI (1:3), as compared with β-CD, is evidenced by the lower magnitude of the 1:1 binding constant (K = 19.6 M^{-1}; cf. Table 2) and is consistent with the decolourization effects concluded by Bertau and Jorg.

Fig. 3 outlines the amount of phth removed (%) from solution by glucose and glucose:CDI (1:3) copolymer. The decolourization of phth by each adsorbent material is very similar and the attenuation of the absorbance of phth is attributed to the presence of glucose; however, the linker is concluded to contribute negligibly. The mole content of pure glucose exceeds that of glucose:CDI (1:3), and therefore, shows an apparently greater decolourization effect. Thus, the results in Figs. 2 and 3 support that the interaction between glucose and phth results in an attenuation of the dye absorbance through a non-inclusion interaction, whereas; the linker (CDI) molecule does not contribute any significant decolourization.

3.3. Calculation of the β-CD/phth 1:1 binding constant ($K_{1:1}$)

Fig. 4 illustrates a typical plot of absorbance vs. $C_{\beta\text{-CD}}$ for a fixed concentration of phth. The line through the data points represents the calculated absorbance values obtained from the NLLS fitting procedure (cf. Eq. (4)). The sharp decrease in absorbance as the $C_{\beta\text{-CD}}$ increases represents the formation of the β-CD/phth complex since the molar absorptivity of the latter is regarded as zero (Buvari et al., 1983; Taguchi, 1986; Eftink et al., 1989). The calculated curves through the experimental data represent the best-fit NLLS curve corresponding to a 1:1 equilibrium binding model. The average 1:1 equilibrium binding constant (K_1) for the β-CD/phth complex binding is estimated as $K_1 = 2.66 \pm 0.3 \times 10^4$ M^{-1} with a standard error of 7.0% from four independent experimental trials.

Table 1
Elemental analysis (C, H, N) results for β-CD, glucose, and the corresponding copolymers at 1:1, 1:2, and 1:3 β-CD:linker reactant ratios.

Material	Theoretical[a]			Experimental			Solvent/water mixture%
	%C	%H	%N	%C	%H	%N	
β-CD	38.4	6.90	0.00	38.2	6.81	0.00	11.6
Glucose	36.4	7.12	0.00	35.9	7.24	0.00	6.65
Glucose:CDI (1:3)	31.9	4.09	4.37	59.8	8.18	8.03	0.841
β-CD:HDI (1:1)	46.1	6.34	6.89	41.8	6.99	2.68	0.874
β-CD:HDI (1:2)	47.4	6.44	3.81	43.0	6.68	3.73	0.700
β-CD:HDI (1:3)	48.4	6.52	5.13	44.0	6.89	5.00	0.633
β-CD:CDI (1:1)	49.0	6.64	2.00	45.3	7.25	2.31	0.889
β-CD:CDI (1:2)	52.1	6.92	3.38	46.6	7.25	3.03	0.607
β-CD:CDI (1:3)	54.4	7.13	4.37	49.0	7.51	3.87	0.302
β-CD:MDI (1:1)	49.4	5.82	2.02	43.4	6.21	3.70	0.569
β-CD:MDI (1:2)	52.9	5.55	3.43	51.1	5.73	4.21	0.846
β-CD:MDI (1:3)	55.4	5.34	4.46	52.6	5.90	4.50	0.645
β-CD:PDI (1:1)	46.4	5.76	2.16	41.4	6.20	2.37	1.09
β-CD:PDI (1:2)	47.9	5.40	3.85	45.5	5.75	2.90	0.875
β-CD:PDI (1:3)	49.1	5.12	5.20	44.6	5.43	4.90	1.16
β-CD:NDI (1:1)	48.2	5.69	2.08	40.5	6.01	0.76	0.990
β-CD:NDI (1:2)	51.0	5.31	3.6	46.5	5.60	3.68	1.60
β-CD:NDI (1:3)	53.1	5.02	4.76	54.4	5.64	7.47	1.63

[a] Based on the synthetic feed ratios used in synthesis of polymer material. β-CD and glucose theoretical compositions were corrected for the amount of hydrate water whereas results for polymeric materials are uncorrected.

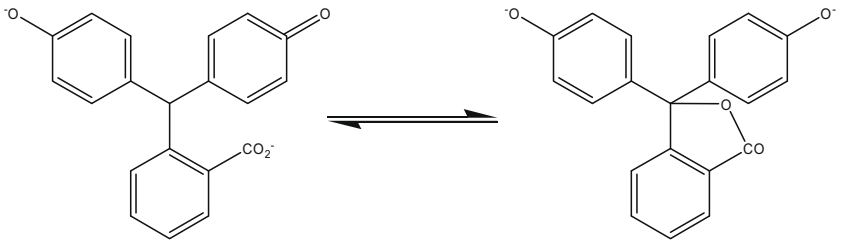

Scheme 2. The molecular structure of the two equilibrium forms of the red colored phenolphthalein dianion in aqueous solution at pH 10.5. The left hand structure represents the quinoid form and the right hand structure is the benzenoid dianion form of phenolphthalein.

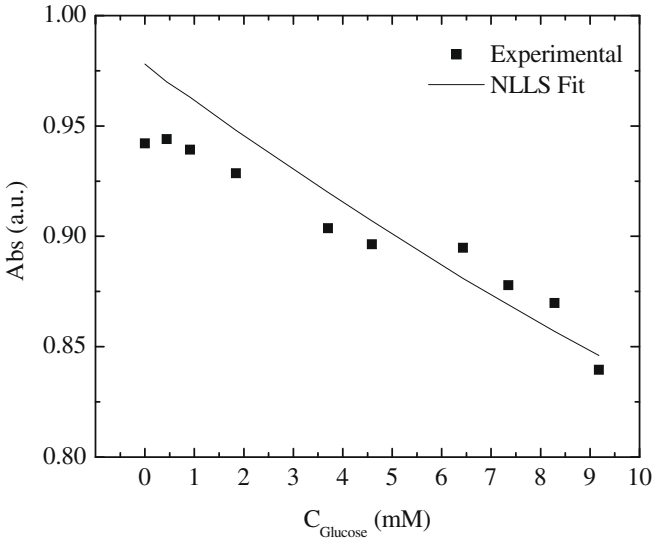

Fig. 2. Phenolphthalein sorption with variable amount of insoluble glucose:CDI (1:3) polymer at 295 K and pH 10.5 in 0.1 M $NaHCO_3$ buffer solution. The solid line refers to the NLLS best-fit according to Eq. (4).

The latter result is in good agreement with independent estimates (Bender & Komiyama, 1978; Buvari et al., 1983; Eftink et al., 1989; Sasaki et al., 1989; Gray et al., 1995).The conditions employed, here, utilized lower ethanol compositions than those of Selvidge and Eftink and the value of K_1 obtained is correspondingly higher.

Fig. 5 represents a plot of Abs. vs. $C_{Glucose}$ at a fixed concentration of phth. In contrast to the results obtained for β-CD, Fig. 5 shows a more gradual decrease in absorbance for glucose and indicates that it has an attenuated binding constant, as compared with β-CD. The maximum absorbance change for glucose was ~15% and the estimated 1:1 binding constant value from NLLS fitting procedure was 15.7 M^{-1}. This relatively weak non-inclusion binding is attributed to H-bonding between glucose and phth, as described above (Bertau & Jorg, 2004).

3.4. Sorption of phth with CD polymers

The decolourization of phth increased as the relative amount of CD polymer was increased for a constant value of C_{phth}. The decolourization results provide support that phth forms 1:1 inclusion complexes between phth and β-CD within the polymer framework. The results from Fig. 3 indicate that non-inclusion and H-bonding interactions with glucose contribute to some decolourization of phth (Bertau & Jorg, 2004); however, the effect is small in comparison with the observed inclusion effect for β-CD (cf. Fig. 4).

Fig. 6a–e illustrates the removal of unbound phth *vs*. the mass of β-CD copolymer materials. In Fig. 6a, the β-CD:HDI copolymer (1:1) shows substantial removal of phth, as shown by the sharp asymptotic increase in bound phth, whereas; the 1:2 and 1:3 materials are incrementally less effective in removing phth from

Table 2
Phenolphthalein based estimates (%) of the surface accessible β-CD site in -cyclodextrin urethane copolymer materials.

Material	β-CD:linker synthetic ratio	$\beta\text{-CD}_{total}$ (mol%)	K_1 (M^{-1})	Accessible β-CD (%)[a]
β-CD	–	100	$2.66(0.3) \times 10^4$	100
Glucose	–	0	15.7	5.91×10^{-2}
Glucose:CDI	1:3	0	17.0	6.39×10^{-2}
β-CD:HDI	1:1	87.1	$2.66(0.3) \times 10^4$	106
	1:2	77.1	$2.66(0.3) \times 10^4$	66.7
	1:3	69.2	$2.66(0.3) \times 10^4$	4.78
β-CD:CDI	1:1	81.2	$2.66(0.3) \times 10^4$	33.2
	1:2	68.4	$2.66(0.3) \times 10^4$	2.03
	1:3	59.1	$2.66(0.3) \times 10^4$	1.04
β-CD:MDI	1:1	81.4	$2.66(0.3) \times 10^4$	38.0
	1:2	69.4	$2.66(0.3) \times 10^4$	31.6
	1:3	60.2	$2.66(0.3) \times 10^4$	18.6
β-CD:PDI	1:1	87.6	$2.66(0.3) \times 10^4$	68.3
	1:2	78.0	$2.66(0.3) \times 10^4$	57.4
	1:3	70.3	$2.66(0.3) \times 104$	14.1
β-CD:NDI	1:1	84.4	$2.66(0.3) \times 10^4$	77.6
	1:2	73.0	$2.66(0.3) \times 10^4$	39.2
	1:3	68.4	$2.66(0.3) \times 10^4$	24.2

[a] Accessible -CD (%) = (β-CD/phth/$\beta\text{-CD}_{total}$) × 100%.

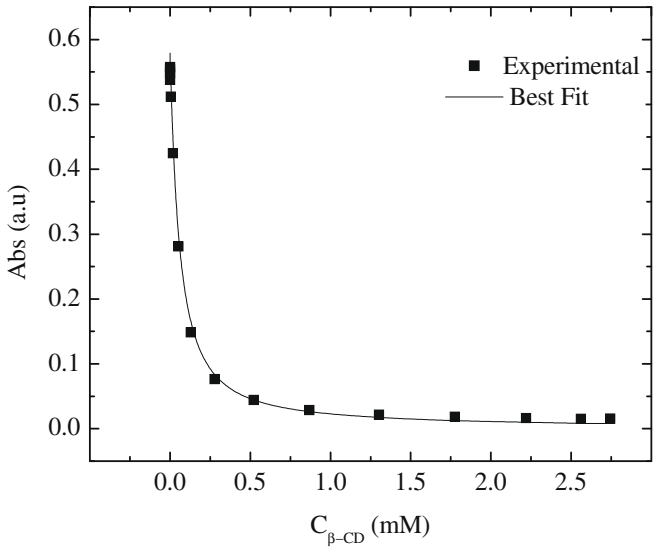

Fig. 4. Absorbance (Abs) of phenolphthalein with variable concentration of β-CD ($C_{\beta\text{-CD}}$) in its native form in aqueous 0.1 M $NaHCO_3$ buffer solution at pH 10.5 and 295 K. The solid line refers to the NLLS best-fit according to Eq. (4).

aqueous solution. The attenuation of phth removal is evident according to the estimates of the accessible β-CD (%) for the 1:1 (∼100%), 1:2 (66.7%), and 1:3 (4.78%) copolymer materials, in accordance with the reduced accessibility of the β-CD inclusion sites. The greater removal of phth implies that phth forms 1:1 complexes with the β-CD inclusion sites in the polymer framework and results in decolourization of the dye. Increasing the cross link density may reduce the sorption properties of the polymeric materials for two possible reasons; (i) steric crowding of the hydroxyl annular region of β-CD, and (ii) attenuated access to the pore framework and β-CD inclusion sites due to an increased cross link density. According to the space filling models of Taguchi, inclusion of the benzenoid form of phth (cf. Scheme 2) as well as the H-bonding between the phenolate ions and the hydroxyl groups of β-CD are required to form the transparent 1:1 β-CD/phth dianion inclusion complex (cf. Scheme 2; Taguchi, 1986). Increased substitution at the β-CD annular region inhibits favourable H-bonding and inclusion binding between β-CD and phth. Thus, the anticipated steric effects are consistent with the attenuated decolourization of phth in highly cross linked materials, as observed in Fig. 6a–e. In addition, copolymers with greater cross link density result in reduced access of phth to the microporous domains of the copolymer framework and result in reduced phth removal because of steric restrictions to the β-CD inclusion sites.

In Fig. 6b, the β-CD:CDI (1:1) copolymer displayed the greatest removal of phth and the 1:2 and 1:3 materials show a reduced effect. A comparison of CDI and HDI linkers indicates that the former is a bulkier linker molecule, and the anticipated steric effects of CDI are more pronounced compared to the results for HDI (Fig. 6a). Fig. 6c–e depicts the removal efficiency for three polymeric materials containing aromatic linker molecules (MDI, PDI, and NDI) at variable reactant mole ratios. In each case, similar sorption of phth

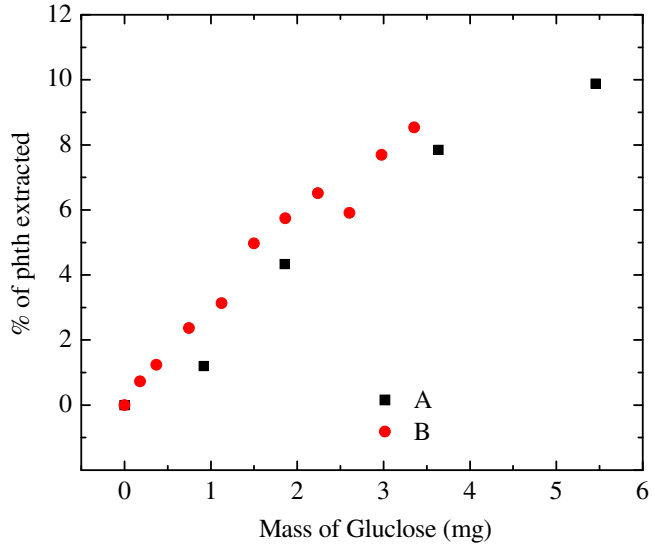

Fig. 3. Phenolphthalein removal (decolourization) from solution using with variable amount of material at 295 K and pH 10.5 in 0.1 M $NaHCO_3$ buffer solution at fixed concentration of phth (3×10^{-5} M); (A) D-(+)-glucose, and (B) glucose:CDI (1:3) copolymer.

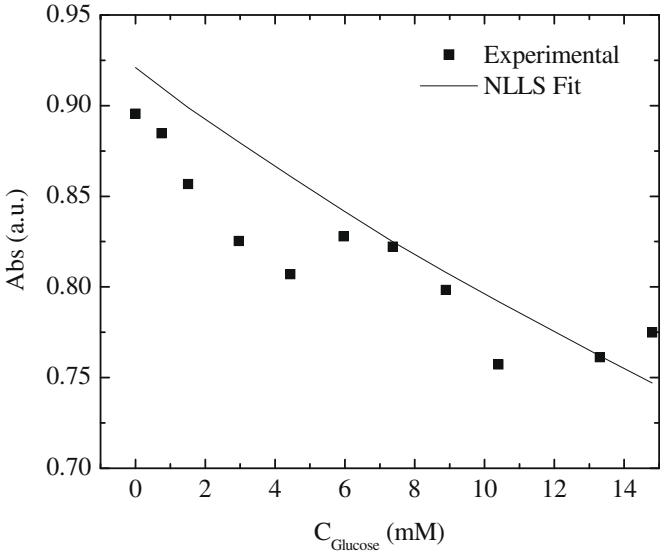

Fig. 5. Phenolphthalein sorption with variable amount of glucose at 295 K and pH 10.5. The solid line refers to the NLLS best-fit according to Eq. (4).

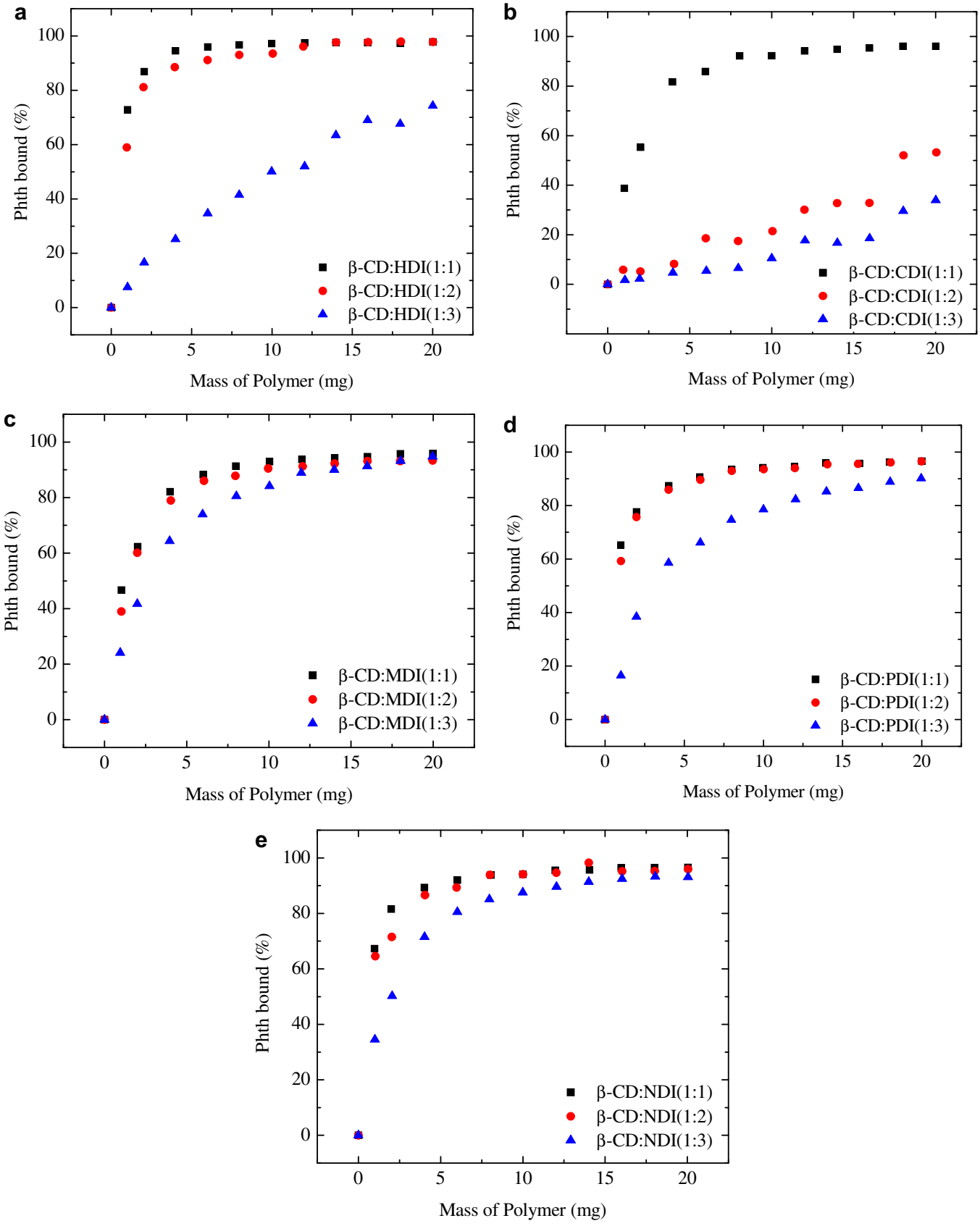

Fig. 6. Percentage of phenolphthalein bound from aqueous solution with β-CD based copolymers vs. polymer mass (mg) in 0.1 M $NaHCO_3$ buffer at pH 10.5 and 295 K: (a) β-CD:HDI, (b) β-CD:CDI, (c) β-CD:MDI, (d) β-CD:PDI, and (e) β-CD:NDI at 1:1, 1:2, and 1:3 reactant mole ratios, respectively.

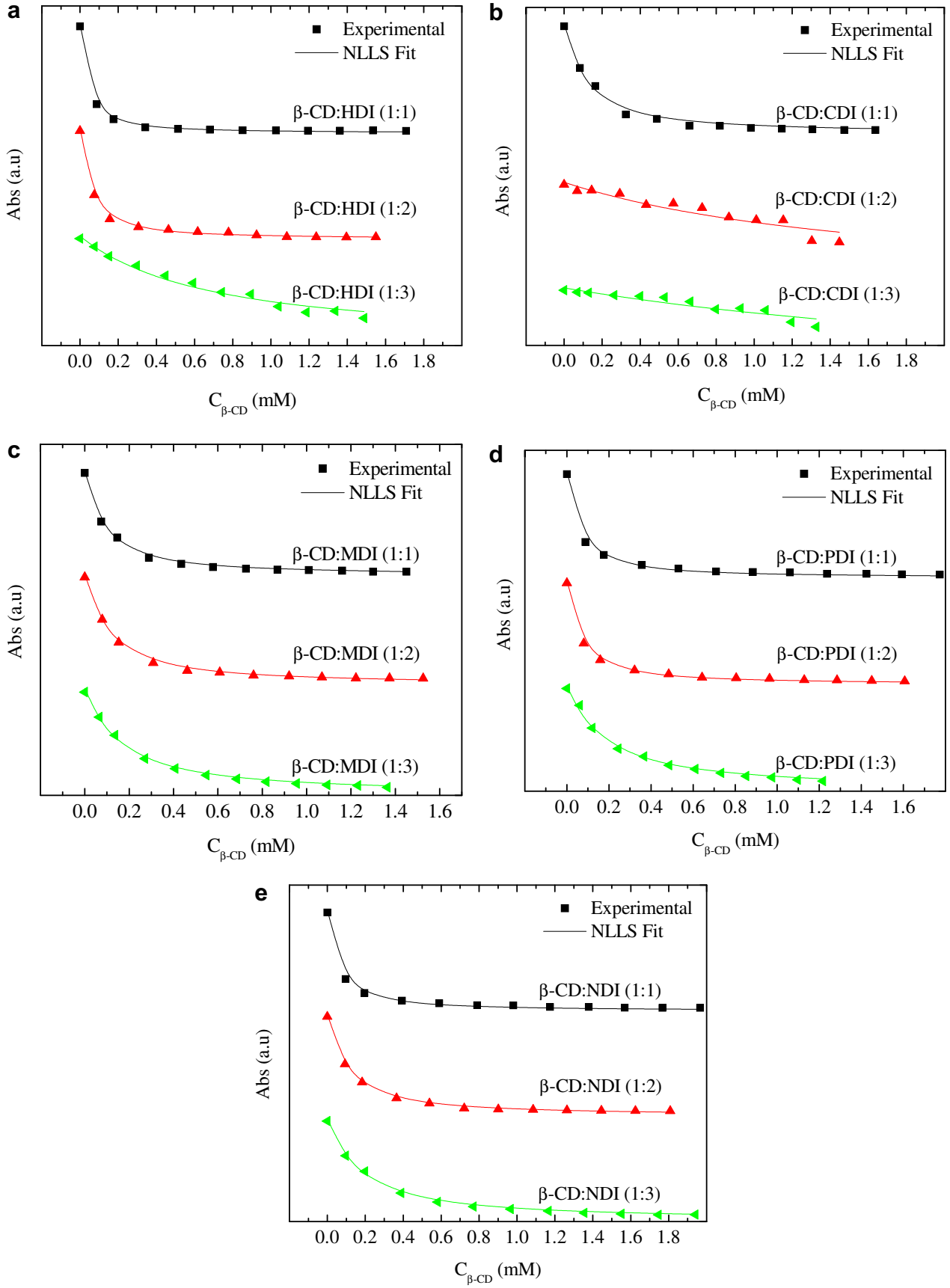

Fig. 7. Absorbance changes for phenolphthalein as a function of increased mole content of β-CD ($C_{β\text{-CD}}$) for various insoluble copolymers at variable synthetic feed ratios at pH 10.5 in 0.1 M $NaHCO_3$ and 295 K: (a) β-CD:HDI, (b) β-CD:CDI, (c) β-CD:MDI, (d) β-CD:PDI, and (e) β-CD:NDI. The solid line refers to the NLLS best-fit according to Eq. (4) where $K_1 = 2.66 \times 10^4\ M^{-1}$ and the fraction bound of β-CD (CD-phth) is an adjustable parameter between 0 to 100 mol%.

is observed for the 1:1 and 1:2 materials; however, complex formation is severely attenuated for the 1:3 copolymers. Steric effects are anticipated between phth and the annular hydroxyl groups of β-CD and domains containing the β-CD inclusion sites at greater cross link ratios. In general, an increase in the linker composition of the copolymers results in significant reduction to the inclusion binding of β-CD and phth, as shown by the different profiles shown in Fig. 6a–e.

Fig. 7a–e illustrate the change in absorbance (Abs) of phth vs. $C_{\beta\text{-CD}}$ for β-CD copolymers at a fixed concentration of phth (C_{phth}). The solid lines through the experimental data represent the calculated Abs values according to the NLLS fitting routine, according to Eq. (4). The decrease in Abs as $C_{\beta\text{-CD}}$ increases is more gradual as the linker ratio content increases for all copolymers studied. In the case of CDI (Fig. 7b), the rapid falloff is less evident and indicates that inclusion binding of phth is reduced even at intermediate (1:2) linker ratios. The greatest attenuation of phth binding is observed at the highest (1:3) linker content for both the aliphatic (*i.e.* HDI and CDI) and aromatic (NDI, PDI, and MDI) linkers. The steric effect appears to correlate with the approximate size of the linker. The decolourization of phth by the 1:1 copolymer materials is listed in descending order as follows: HDI > NDI > PDI > MDI ≈ CDI. This observation suggests that the relative size of the linker plays a steric role in affording accessibility to the β-CD inclusion sites within the polymeric framework. Fig. 7a and b illustrate the behaviour for copolymers with aliphatic linkers while Fig. 7c–e shows results for copolymers with aromatic linkers. It is important to note that the aliphatic and aromatic linkers are anticipated to exhibit differences in their conformational rigidity. Thus, aromatic linkers such as NDI and MDI may form more open pore structures within the polymer framework. Flexible aliphatic linkers such as HDI and CDI may form compact frameworks because their variable conformations may result in a collapsed framework structure. This hypothesis is supported by the attenuated access to the inclusion sites for phth, as evidenced by the results shown in Figs. 6 and 7. There appears to be a compromise between steric crowding in the annular hydroxyl region of β-CD vs. the creation of accessible pore structures within the framework as the relative size and rigidity of the linker increases.

Scheme 3 outlines the effect of increasing the degree of substitution in the annular hydroxyl region of β-CD for a diisocyanate linker over the range of β-CD:linker mole ratios (1:1, 1:2, and 1:3) studied in this work. At the 1:1 ratio, the primary hydroxyl groups of the β-CD are more reactive as compared with the secondary hydroxyl groups. In the case of bulky diisocyanates, the estimated number of substituents in the annular hydroxyl region is estimated *ca.* three substituents per annular face (cf. Scheme 3) and this has been independently supported elsewhere (Martel, Leckchiri, Pollet, & Morcellet, 1995; Weickenmeier & Wenz, 1996; Glazyrin, Grachev, Kurochkina, & Nifant'ev, 2004;Yuan, Jin, & Li, 2008). Once steric crowding occurs at the narrow end of the β-CD annulus, linkers react at the wider secondary annular region until the degree of substitution approaches ∼3. Scheme 3 illustrates the distribution of substituents from left to right (a–c) in accordance with the β-CD:linker reactant ratio from 1:1 to 1:3, respectively. The accessibility of inclusion sites presented in Table 2 support this hypothesis since relatively high accessibility is observed at the 1:1 reactant ratio. According to Taguchi, the formation of the 1:1 β-CD/phth inclusion complex occurs by inclusion of the benzenoid form of phth (cf. Scheme 2) and H-bonding between the two phenoxide anions and the secondary annular hydroxyl groups located at the wide end of the β-CD annulus (cf. Scheme 2; Buvari et al., 1983). According to Glazyrin et al., a study of various modified forms of β-CD indicated that a four- to 40-fold decrease in the 1:1 binding constant was observed for acetylated and hydroxypropyl substituted β-CD where the average degree of substitution reaches ∼3.8 and 3.6, respectively. They concluded that the binding of β-CD and some of its water-soluble derivatives may form complexes with phth depending on the structure, substitution position, and degree of substitution at the 2-, 3-, and 6-hydroxyl positions, respectively.

3.5. Accessibility of β-CD inclusion binding sites in the polymers

The estimation of accessible inclusion binding sites of β-CD requires certain assumptions: (i) polymers possess variable accessibility due to differences in the cross link density, (ii) phth binds exclusively to β-CD as a 1:1 inclusion complex where the molar absorptivity of bound phth is zero, and (iii) the 1:1 binding constant is assumed to be similar to that of native β-CD in the absence of steric effects. The third assumption is supported from experiments that compare the binding between glucose and glucose based polymers. It was concluded that the urethane linkage does not affect the magnitude of the 1:1 binding constant for glucose-CDI copolymers. The presence of available hydroxyl groups affects the decolourization of phth as observed in aqueous solutions containing glucose and the results obtained here are also supported by the conclusions of Bertau and Jorg.

The percentage of the accessible β-CD was calculated by varying the percentage of bound β-CD (varying [CD-phth] in Eq. (2)–(4)) for copolymers containing β-CD. The best-fit between the calculated Abs and experimental values (cf. Fig. 7a–e) provided estimates of the accessible inclusion sites. Eq. (4) was used with a fixed value of K_1 for the polymeric materials, similar to that obtained for the 1:1 β-CD/phth complex. Table 2 shows the estimates of the surface accessible β-CD for each copolymer at different synthetic ratios.

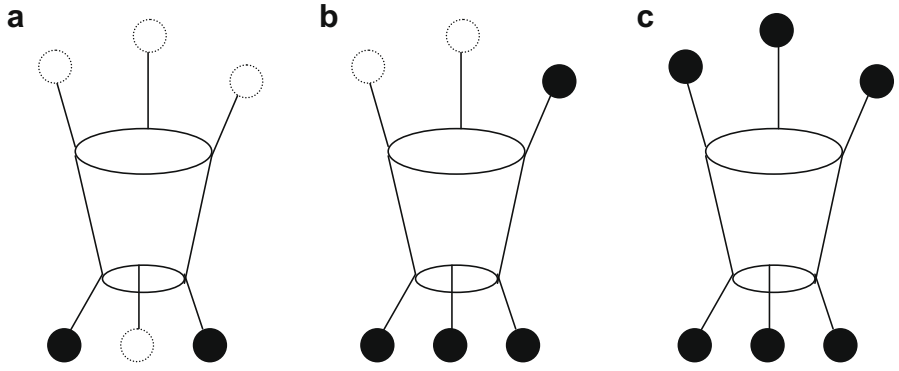

Scheme 3. Illustration of the sites of substitution of diisocyanate cross linker units to the primary (narrow end) and secondary (wide end) hydroxyl groups in the annular regions of a β-CD copolymer: (a) β-CD:linker (1:1), and (b) β-CD:linker (1:2), and (c) β-CD:linker (1:3) reactant ratios. The solid spheres represent covalently attached sites and open spheres represent available (unreacted) sites.

Table 3
Fractional coverage, θ[a], at 1 mg of the polymer and Gibbs free energy change[b], ΔG° of complex formation with phth in aqueous solution at pH 10.5 and 295 K.

Polymer	Ratio β-CD:linker	
	1:1 (θ, ΔG°, kJ/mol)	1:2 (θ, ΔG°, kJ/mol)
HDI	0.773, −29.7	0.741, −28.7
CDI	0.619, −27.0	NR[c]
MDI	0.838, −28.3	0.818, −28.3
PDI	0.633, −27.9	0.501, −27.3
NDI	0.598, −28.4	0.500, −26.7

[a] θ – refer to Eq. (6).
[b] ΔG° – refer to Eq. (7).
[c] NR – not reported because the surface accessibility was too low resulting in poor fits according to the Sips isotherm model (cf. Eq. (5)).

The accessibility of the inclusion sites decreases as the cross link density increases. The relative ordering of the steric effects at high cross link density correlates inversely with the size of the linker as follows: HDI > CDI > PDI > MDI ≈ NDI. Steric crowding and the reduction of the pore volume within the framework are anticipated to retard the 1:1 inclusion complex formation between β-CD and phth. Polymers with low cross link density such as the β-CD:HDI (1:1) copolymer possesses the greatest inclusion accessibility whereas the β-CD:CDI (1:3) copolymer has the lowest accessibility values. The linker domains within the framework do not contribute to complex formation with phth to any appreciable extent (cf. Fig. 3) as shown by the minor decolourization effect of the glucose-CDI polymer is less than 0.1% (cf. Table 2).

Table 3 lists the Gibbs free energy change of complex formation (ΔG°) and provides independent support for the comparable 1:1 binding constants of the native β-CD/phth complex and β-CD copolymer/phth complexes. The reasonable fit obtained using the Sips model instead of the Langmuir ($n_s = 1$) model suggests that the linkers may affect the decolourization of phth, albeit limited. However, the formation of the 1:1 inclusion complexes between β-CD based copolymers and phth is the predominant mechanism responsible for the observed decolourization. In Table 3, the site occupancy decreased as the cross linking density increases, and correlates with the decreased accessibility of the inclusion sites. The Gibbs free energy change depends on the site occupancy of the sorption sites where they are directly proportional to the amount of accessible β-CD. Moreover, the magnitude of ΔG° for the copolymers is slightly greater than the ΔG° of the 1:1 β-CD/phth complexes (∼−25 kJ/mol) (Wilson et al., 1997; Mohamed et al., 2009). The slight differences in ΔG° may be due to differences in hydration and steric effects because of cross linking in the β-CD copolymers, as suggested by Glazyrin et al.

4. Conclusions

In this research we report the results of a dye-based study of water insoluble β-CD based copolymer sorbents in aqueous solution at pH 10.5 and 295 K. In contrast to other design strategies that employ relatively high β-CD:linker reactant ratios, the copolymers in this study utilized relatively low ratios (1:1 to 1:3), and yet, the surface accessibility was remarkably different for the five sets of copolymer sorbent materials. The copolymer surface accessibility of the β-CD inclusion sites ranged between 1% and 100%, as evidenced by the formation of 1:1 β-CD/phth inclusio complexes. The Gibbs free energy change for the formation of 1:1 complexes between phth and β-CD copolymer materials ranged between -27 to -30 kJ mol^{-1}, according to the Sips isotherm model.

This paper represents the first systematic and quantitative analysis of β-CD inclusion sites in urethane copolymer materials. The dye based sorption method presented herein represents a facile and relatively low cost analytical method for β-CD based copolymer materials. This method relies on the specific molecular recognition between β-CD and phenolphthalein, and it provides useful results about the sorption properties of β-CD based sorbent materials. We propose the use of phth as an inclusion selective guest and versatile optical probe for β-CD based copolymer sorbent materials. The molecular selectivity of this dye based method will contribute to the design of novel types of β-CD based materials for sorption based applications involving the inclusion binding of adsorbates from solution and gas phase media, respectively.

Acknowledgments

Financial assistance was provided by the Natural Sciences and Engineering Research Council and the Program of Energy Research and Development. M.H.M acknowledges the University of Saskatchewan for the award of a Graduate Teaching Fellowship and Environment Canada for the Science Horizons Program award. Mr. Joel Hardes is acknowledged for his helpful technical assistance.

References

Bender, M. L., & Komiyama, M. (1978). *Cyclodextrin chemistry*. Berlin: Springer-Verlag.
Bergamasco, R. C., Zanin, G. M., & Moraes, F. F. (2007). Grafting of cyclodextrins onto filter paper. *Journal of Inclusion Phenomena and Macrocyclic Chemistry, 57*(1–4), 75–78.
Bertau, M., & Jorg, G. (2004). Saccharides as efficacious solubilisers for highly lipophilic compounds in aqueous media. *Bioorganic & Medicinal Chemistry, 12*(11), 2973–2983.
Burckbuchler, V., Wintgens, V., Leborgne, C., Lecomte, S., Leygue, N., Scherman, D., et al. (2008). Development and characterization of new cyclodextrin polymer-based DNA delivery systems. *Bioconjugate Chemistry, 19*(12), 2311–2320.
Buvári, Á., & Barcza, L. (1979). Ɓ-Cyclodextrin complexes of different type with inorganic compounds. *Inorganica Chimica Acta, 33*(2), L179–L180.
Buvári, Á., Barcza, L., & Kajtár, M. J. (1988). Complex formation of phenolphthalein and some related compounds with β-cyclodextrin. *Journal of the Chemical Society, Perkin Transactions, 2*, 1687–1690.
Buvari, A., Szejtli, J., & Barcza, L. (1983). *Journal of Inclusion Phenomena, 1*(2), 151–157.
Crini, G. (2005). Recent developments in polysaccharide-based materials used as adsorbents in wastewater treatment. *Progress in Polymer Science, 30*, 38–70.
Crini, G., Bertini, S., Torri, G., Naggi, A., Sforzini, D., Vecchi, C., et al. (1998). Sorption of aromatic compounds in water using insoluble cyclodextrin polymers. *Journal of Applied Polymer Science, 68*(12), 1973–1978.
Dharmawardana, U. R., Christian, S. D., Tucker, E. E., Taylor, R. W., & Scamehorn, J. F. (1993). A surface tension method for determining binding constants for cyclodextrin inclusion complexes of ionic surfactants. *Langmuir, 9*(9), 2258–2263.
Donze, C., Chatjigakis, A., & Coleman, A. W. (1992). Co-solvent modulation of the inclusion selectivity of β-cyclodextrin. *Journal of Inclusion Phenomena and Molecular Recognition in Chemistry, 13*(2), 155–161.
Eftink, M. R., Andy, M. L., Bystrom, K., Perlmutter, H. D., & Kristol, D. S. (1989). Cyclodextrin inclusion complexes: studies of the variation in the size of alicyclic guests. *Journal of the American Chemical Society, 111*(17), 6722–6765.
Fontananova, E., Di Profio, G., Curcio, E., Giorno, L., & Drioli, E. (2007). Functionalization of polymeric membranes by impregnation and in situ cross-linking of a PDMS/β-cyclodextrin network. *Journal of Inclusion Phenomena and Macrocyclic Chemistry, 57*(1–4), 537–543.
Fourmentin, S., Surpateanu, G. G., Blach, P., Landy, D., Decock, P., & Surpateanu, G. (2006). Experimental and theoretical study on the inclusion capability of a fluorescent indolizine β-cyclodextrin sensor towards volatile and semi-volatile organic guest. *Journal of Inclusion Phenomena and Macrocyclic Chemistry, 55*(3–4), 263–269.
Gelb, R. I., Schwartz, L. M., Cardelino, B., & Laufer, D. A. (1980). The complexation chemistry of cycloamyloses: equilibrium constants by novel spectrophotometric methods. *Analytical Biochemistry, 103*(2), 362–368.
Georgiou, M. E., Georgiou, C. A., & Koupparis, M. A. (1995). Flow injection gradient technique in spectrophotometric determination of formation constants of micromolecule-cyclodextrin complexes. *Analytical Chemistry, 67*, 114–123.
Glazyrin, A. E., Grachev, M. K., Kurochkina, G. I., & Nifant'ev, E. E. (2004). Inclusion compounds of some water-soluble β-cyclodextrin derivatives with phenolphthalein. *Russian Journal of General Chemistry, 74*(12), 1922–1925.
Gray, J. E., MacLean, S. A., & Reinsborough, V. C. (1995). Limitations of the phenolphthalein competition method for estimating cyclodextrin binding constants. *Australian Journal of Chemistry, 48*(3), 551–556.
Harada, A., Hashidzume, A., & Takashima, Y. (2006). Cylodextrin-based supramolecular polymers. *Advances in Polymer Science, 201*, 1–43.

Harrison, J. C., & Eftink, M. R. (1982). Cyclodextrin-adamantanecarboxylate inclusion complexes: a model system for the hydrophobic effect. *Biopolymers, 21*(6), 1153–1166.

Janus, L., Crini, G., El-Rezzi, V., Morcellet, M., Cambiaghi, A., Torri, G., et al. (1999). New sorbents containing beta-cyclodextrin. Synthesis, characterization, and sorption properties.. *Reactive & Functional Polymers, 42*(3), 173–180.

Junquera, E., Tardajos, G., & Aicart, E. (1993). Effect of the presence of β-cyclodextrin on the micellization process of sodium dodecyl sulfate or sodium perfluorooctanoate in water. *Langmuir, 9*(5), 1213–1219.

Landy, D., Fourmentin, M. S., & Surpateanu, G. (2000). Analytical improvement in measuring formation constants of inclusion complexes between β-cyclodextrin and phenolic compounds. *Journal of Inclusion Phenomena and Macrocyclic Chemistry, 38*(1–4), 187–198.

Liu, Y., & Liu, Y.-J. (2008). Biosorption isotherms, kinetics and thermodynamics. *Separation and Purification Technology, 61*(3), 229–242.

Martel, B., Leckchiri, Y., Pollet, A., & Morcellet, M. (1995). Cyclodextrin-poly(vinylamine) systems. I. Synthesis, characterization and conformational properties.. *European Polymer Journal, 31*(11), 1083–1088.

Meier, M. M., Luiz, M. T. B., Farmer, P. J., & Szpoganicz, B. (2001). The influence of β- and γ-cyclodextrin cavity size on the association constant with decanoate and octanoate anions. *Journal of Inclusion Phenomena and Macrocyclic Chemistry, 40*(4), 291–295.

Mohamed, M. H., Wilson, L. D., Headley, J. V., & Peru, K. M. (2008). Novel materials for environmental remediation of tailing pond waters containing naphthenic acids. *IChemE: Process Safety and Environment Protection, 86*(4), 237–243.

Mohamed, M. H., Wilson, L. D., Headley, J. V., & Peru, K. M. (2009). A Spectral displacement study of cyclodextrin/naphthenic acids inclusion complexes. *Canadian Journal of Chemistry, 87*, 1747–1756.

Rossi, R. H., Silva, O. F., Vico, R. V., & Gonzalez, C. J. (2009). Molecular organization and recognition properties of amphiphilic cyclodextrins. *Pure and Applied Chemistry, 81*(4), 755–765.

Saint Aman, E., & Serve, D. (1990). A conductimetric study of the association between cyclodextrins and surfactants – application to the electrochemical study of a mixed aqueous system: substrate, cyclodextrin, surfactant. *Journal of Colloid and Interface Science, 138*(2), 365–375.

Sasaki, K. J., Christian, S. D., & Tucker, E. E. (1989). Study of the stability of 1:1 complexes between aliphatic alcohols and β-cyclodextrin in aqueous solution. *Fluid Phase Equilibria, 49*, 281–289.

Schuette, J. M., & Warner, I. M. (1994). Interaction of fluorinated alcohols with the β-cyclodextrin/acridine complex. *Analytical Letters, 27*(6), 1175–1182.

Selvidge, L. A., & Eftink, M. R. (1986). Spectral displacement techniques for studying the binding of spectroscopically transparent ligands to cyclodextrins. *Analytical Biochemistry, 154*(2), 400–408.

Sips, R. (1948). Structure of catalyst surface. *Journal of Chemical Physics, 16*, 490–495.

Suzuki, I., & Yamauchi, A. (2006). Pseudo[3]rotaxane type complexation between α- and β-cyclodextrins and *N*,*N*′-diheptyl-4,4′-bipyridinium. *Journal of Inclusion Phenomena and Macrocyclic Chemistry, 54*(3–4), 193–200.

Taguchi, K. (1986). Transient binding of phenolphthalein-β-cyclodextrin complex: an example of induced geometrical distortion. *Journal of the American Chemical Society, 108*(10), 2705–2709.

Topchieva, I. N., Kalashnikov, F. A., Spiridonov, V. V., Mel'kinov, A. B., Polushina, G. E., & Lezov, A. V. (2003). Cyclodextrin-containing nanotubes as a base for designing materials with a new architecture. *Doklady Chemistry, 390*(1–3), 115–118.

Tutaj, B., Kasprzyk, A., & Czapkiewicz, J. (2003). The Spectral displacement technique for determining the binding constants of β-cyclodextrin – alkyltrimethylammonium inclusion complexes. *Journal of Inclusion Phenomena and Macrocyclic Chemistry, 47*(3–4), 133–136.

Uyar, T., Havelund, R., Nur, Y., Hacaloglu, J., Besenbacher, F., & Kingshott, P. (2009). Molecular filters based on cyclodextrin functionalized electrospun fibers. *Journal of Membrane Science, 332*(1–2), 129–137.

Velaz, I., Isasi, J. R., Sanchez, M., Uzquenda, M., & Ponchel, G. (2007). Structural characteristics of some soluble and insoluble β-cyclodextrin polymers. *Journal of Inclusion Phenomena and Macrocyclic Chemistry, 57*(1–4), 65–68.

Wan Yunus, W. M. Z., Taylor, J., Bloor, D. M., Hall, D. G., & Wyn-Jones, E. (1992). Electrochemical measurements on the binding of sodium dodecyl sulfate and dodecyltrimethylammonium bromide with α- and β-cyclodextrins. *Journal of Physical Chemistry, 96*(22), 8979–8982.

Warner, I. M., & Schuette, J. M. (1993). Spectroscopic studies in cyclodextrin solutions. *Advances in Multidimensional Luminescence, 2*, 61–83.

Weickenmeier, M., & Wenz, G. (1996). Cyclodextrin side chain polyesters. Synthesis and inclusion of adamantane derivatives. *Macromolecular Rapid Communications, 17*(10), 731–736.

Wenz, G. (1994). Cyldoextrins as building blocks for supramolecular structures and functional units. *Angewandte Chemie International Edition in English, 33*(8), 803–822.

Wilson, L. D., Siddall, S. R., & Verrall, R. E. (1997). A spectral displacement study of the binding constants of cyclodextrin-hydrocarbon and–fluorocarbon surfactant inclusion complexes. *Canadian Journal of Chemistry, 75*(7), 927–933.

Wintgens, V., & Amiel, C. (2005). Surface plasmon resonance study of the interaction of a β-cyclodextrin polymer and hydrophobically modified poly(*N*-isopropylacrylamide). *Langmuir, 21*(24), 11455–11461.

Wood, D. J., Hruska, F. E., & Saenger, W. (1977). Proton NMR study of the inclusion of aromatic molecules in α-cyclodextrin. *Journal of the American Chemical Society, 99*(6), 1735–1740.

Yuan, C., Jin, Z., & Li, X. (2008). Evaluation of complex forming ability of hydroxypropyl-β-cyclodextrins. *Food Chemistry, 106*(1), 50–55.